ChemComm

COMMUNICATION

View Article Online
View Journal | View Issue

Cite this: *Chem. Commun.*, 2015, **51**, 8284

Received 11th February 2015,
Accepted 3rd April 2015

DOI: 10.1039/c5cc01306b

www.rsc.org/chemcomm

Self-assembling corroles†‡

Rafał Orłowski,[ab] Olena Vakuliuk,[ab] Maria Pia Gullo,[c] Oksana Danylyuk,[d] Barbara Ventura,[c] Beata Koszarna,[a] Anna Tarnowska,[b] Nina Jaworska,[ab] Andrea Barbieri*[c] and Daniel T. Gryko*[a]

***trans*-A_2B-corroles bearing $-OCH_2CONHR$ groups at the *ortho* position of the *meso*-phenyl substituent undergo self-organization both in the solid state as well as in solution. The lack of additional donor atoms induces sheet formation, but if the pyridine unit is present in the structure, more complex helical forms are formed.**

Self-assembly as a strategy towards creating large, highly organized structures from relatively simple building blocks is an attractive goal and the design of organic compounds with the ability to adopt specific compact conformations continues to be a flourishing area of research.[1] Among the various possibilities, self-organization of porphyrinoids draws particular attention[2] because these compounds are present in chlorosomes, the simplest yet very efficient cylindrical systems which allow bacteria to harvest low intensity light.[3] While studying chlorosomes comprising of bacteriochlorophyll *c* is rewarding, the complexity of this building block makes it difficult to engineer any modifications. Many *meso*-substituted A_4-porphyrins self-assemble[2] and Balaban and co-workers have proved that porphyrins possessing the minimum number of vantage points can create large organized assemblies as well.[4] It is worth noting that phenylalanine–porphyrin hybrids afforded spherical self-assemblies.[5] We reasoned that employing corroles,[6,7] structurally analogous, yet distinctly different porphyrinoids, could lead to different self-organizing patterns. The only known example of self-assembly of corroles is the amphiphilic sodium salt.[8] We decided to focus on the –NHCO– moiety as a key group, which is responsible for various patterns of self-organization in naturally occurring proteins. The effect of hydrogen-bonding ability of the –NHCO– moiety has been utilized by numerous researchers to form self-assembled structures[9] with the most prominent being Huc's foldamers[10] and Vullev's electrets.[11]

Our design relied on the presence of the OCH_2CONHR functionality at position 2 of the phenyl group located at position 10 of the corrole. We reasoned that placing diverse amide scaffolds in such a manner would create a suitable environment for self-assembly *via* the combination of intermolecular hydrogen bonds and π-stacking. By placing strongly electron-withdrawing pentafluorophenyl groups at positions 5 and 15, we secured the photostability of the designed macrocycles.[6d] The required *trans*-A_2B-corrole **3** was synthesized from aldehyde **1** and 5-(pentafluorophenyl)dipyrrane (**2**) in a HCl–H_2O–MeOH system[12] with 54% yield (Scheme 1).

For the transformation of the ester group into a secondary amide we initially used a finding that esters react with primary aliphatic amines in polar protic solvents without any catalyst.[13] For the model reaction with ethanolamine (**4**), we used a mixture of MeOH and toluene instead of pure MeOH due to solubility issues (Scheme 1). The desired corrole **7** was obtained in 94% yield, but 7 days were required for complete substrate conversion. Faced with long reaction time and inspired by recent reports of various catalysts used in the amination of esters,[14] we performed a short optimization study. In the case of the DBU-mediated reaction,[14a] we achieved complete conversion within 6 hours, while the yield of corrole **7** remained the same. On the other hand, in a reaction carried out in the presence of $La(OTf)_3$ (5 mol%),[14c] we obtained a lower yield[15] (although the reaction time was only 1 hour). Having the optimized conditions in hand (DBU, MeOH, toluene, 6 h), we then prepared two additional amides **8** and **9** from 3-(aminomethyl)pyridine (**5**) and *n*-butylamine (**6**) with comparable yields (Scheme 1).

We made a striking observation during analysis of the ^1H NMR spectra of the obtained corroles. In the spectrum of the parent corrole **3**, the signals did not vary from standard data obtained for this class of compounds with the signal assigned

[a] *Institute of Organic Chemistry, Polish Academy of Sciences, Kasprzaka 44/52, 01-224 Warsaw, Poland. E-mail: dtgryko@icho.edu.pl*
[b] *Warsaw University of Technology, Faculty of Chemistry, Noakowskiego 3, 00-664 Warsaw, Poland*
[c] *Istituto per la Sintesi Organica e la Fotoreattività (ISOF), CNR, Via P. Gobetti 101, 40129 Bologna, Italy. E-mail: andrea.barbieri@isof.cnr.it*
[d] *Institute of Physical Chemistry, Polish Academy of Sciences, Kasprzaka 44/52, 01-224 Warsaw, Poland*

† Dedicated to Prof. Lucia Flamigni on the occasion of her retirement.

‡ Electronic supplementary information (ESI) available: Experimental details for compounds **3** and **7–9**, ^1H NMR and ^{13}C NMR spectra, photophysical data and X-ray crystallographic data for **8** and **9**. CCDC 1048779 and 1048780. For ESI and crystallographic data in CIF or other electronic format see DOI: 10.1039/c5cc01306b

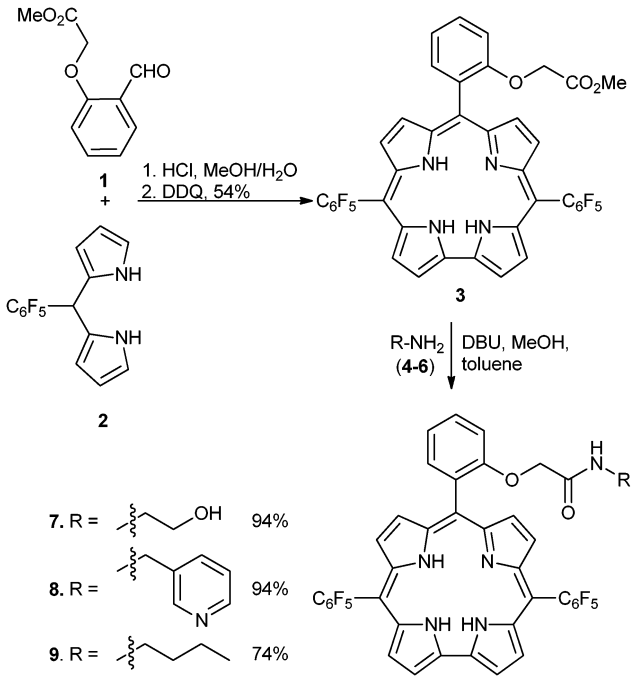

Scheme 1 Synthesis of corroles **3** and **7–9**.

to the –OMe group at 3.47 ppm and that of the inner protons at −2.52 ppm; however, the signals of amides **7–9** were strongly upfield shifted (Fig. S1, ESI‡).

Protons originating from the side chains of the amides were located approximately 2 ppm upfield *vs.* expectations. Pyridine protons were in the range 5–6.5 ppm for corrole **8**, while aliphatic CH_2 was below 0 ppm for corrole **9** (Fig. 1). The macrocyclic ring current of aromatic porphyrinoids is known to cause significant shielding of the inner protons, and thus, this result constituted evidence that, in each case, the amide-arm was located in close proximity to the corrole core. In order to gain better insight into the character of these interactions, we obtained XRD quality crystals for two corroles.

Recrystallization of corroles by vapor diffusion at room temperature from the $CHCl_3$–hexane mixture provided dark purple plates for compounds **8** and **9**, suitable for X-ray crystallographic characterization. Unfortunately, it was not possible to obtain single crystals of corrole **7**. In all crystal structures of

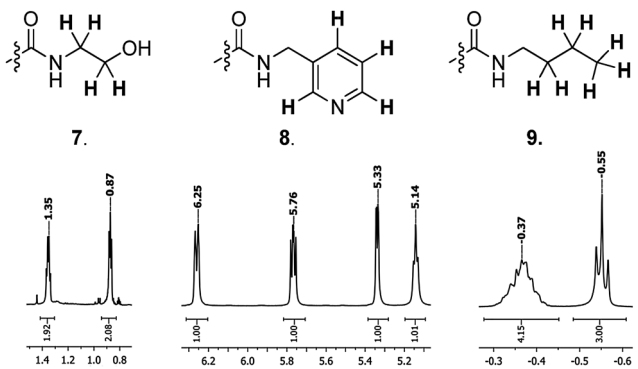

Fig. 1 The key fragments of ^{1}H NMR spectra of corroles **7–9**.

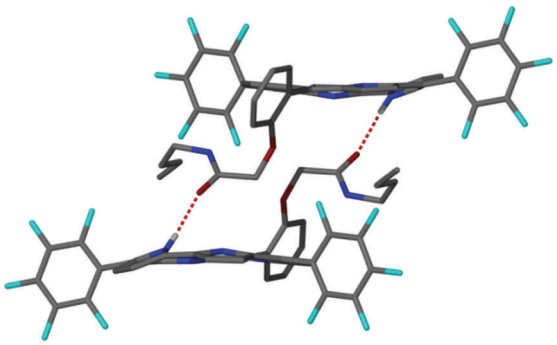

Fig. 2 Crystal structure of **9**·$CHCl_3$. Hydrogen atoms removed for clarity.

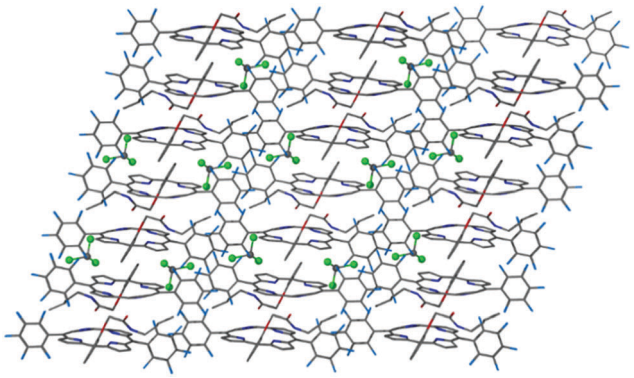

Fig. 3 Hydrogen bonded sheets of **9**.

free-base corrole reported so far, the corrole macrocycle is considerably distorted from planarity because of the steric repulsion between the three inner NH hydrogen atoms.[7a,i,17b,18] The crystal structure of corrole **9** as a chloroform solvate is shown in Fig. 2. One pyrrole ring was tilted up and formed a hydrogen bond to the carbonyl oxygen atom of the side chain of the adjacent corrole (the N–H···O distance 2.80 Å).

The corroles self-assembled into hydrogen-bonded dimers with their side chains sandwiched between two macrocyclic cores (Fig. 2) and they formed large sheets (Fig. 3). The large difference between the interdimer mean planar spacing (3.8 Å) and the intradimer distance (6.8 Å) in the case of corrole **9** indicated that there are no stacking interactions within the hydrogen bonded dimer of this corrole, due to the steric hindrance arising from sandwiching the corrole side chains between the macrocyclic cores.

The crystal structure of corrole **8** as the chloroform solvate is shown in Fig. 4. The change of the side chain had significant influence on the self-assembly of this corrole in the solid state. The pyridyl ring of the side chain was situated above the corrole plane, evidently interacting with the aromatic macrocycle *via* π-stacking. The previously observed (corrole **9**) strong hydrogen bond between NH and amidic C=O was absent. One of the pyrrole rings of the corrole was significantly tilted downward and was hydrogen bonded *via* its pyrrolic NH to the pyridine substituent of the adjacent macrocycle in the crystal lattice (the N–H···N distance 2.88 Å). Such intermolecular interaction led to the formation of a hydrogen bonded helical self-assembly where each corrole

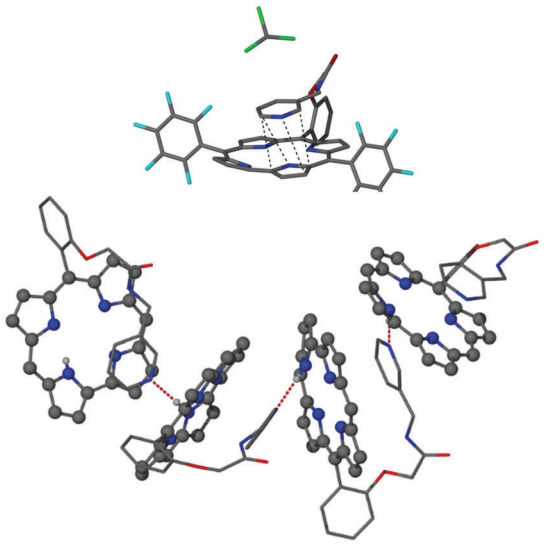

Fig. 4 Crystal structure of **8**·$CHCl_3$ showing intramolecular π–π interactions between the pyridine side chain and the macrocyclic core as well as the hydrogen bonded helical assembly of **8**. Hydrogen atoms and C_6F_5 group were removed for clarity.

interacted with two neighbors acting as a donor (pyrrolic NH) and an acceptor (pyridine nitrogen) of hydrogen bonds (Fig. 4).

UV-vis absorption analysis of the three corroles **3**, **7**, and **9** was performed at room temperature in dilute solutions (c = 5–8 × 10^{-6} M) of dichloromethane, acetonitrile, methanol, and toluene; relevant data are reported in Fig. S1–S4 (ESI‡) and summarized in Table S1 (ESI‡). The molar extinction coefficient values obtained in several solvents are in agreement with those already reported in the literature for similar systems (λ_{max} = 406–417 nm, ε_{max} = 1.1–1.4 × 10^5 M^{-1} cm^{-1} for the Soret band and λ_{max} = 559–570 nm, ε_{max} = 1.6–2.3 × 10^4 M^{-1} cm^{-1} for the first Q bands).[16,17]

Absorption maxima and extinction coefficients were only slightly affected by solvent change. Furthermore, the presence of different groups in the *meso*-aryl unit did not significantly affect the absorption features, probably because of similar modifications to the symmetry of the macrocycles induced by the substituents.

Corroles **3**, **7**, and **9** showed solvent independent emission behavior at room temperature (Fig. S1–S4, ESI‡). All emission spectra displayed intense and structured profiles, composed of one peak at around 650 nm with a shoulder at longer wavelengths as a result of the vibronic progression, and lifetimes between 3.7 and 4.3 ns in all the investigated solvents (Table S2, ESI‡). The photoluminescence quantum yield in methanol, *ca.* 0.13, is lower than in the other solvents, *ca.* 0.15. The slight decrease in methanol could be attributed to intermolecular hydrogen bonding occurring between the solvent hydroxyl group and the CO group on the corrole side chain. This interaction increases k_{nr} through introduction of non-radiative deactivation pathways, as k_r is not affected by the solvent. As already observed in the absorption spectra, the different substituents in the *meso*-phenyl ring on the macrocyclic core did not have distinct effects on the luminescence properties at room temperature. Low temperature measurements evidenced the presence of the typical features of two tautomeric forms T1 and T2, in agreement with literature data (Fig. S5 and Table S3, ESI‡). The peculiar influence of the temperature on emission properties represents an original feature for this class of compounds.[19]

In order to investigate the aggregation properties of corroles **3**, **7**, and **9**, UV-vis absorption and emission spectra were acquired in solvents of different polarity and proticity and in mixtures thereof. In particular, in the attempt to detect the spectroscopic fingerprints of the corrole **9** dimer, we have examined the photophysical behavior of **9** in a $CHCl_3$–hexane mixture (*i.e.* the same solvent mixture used to grow the crystals for XRD) at increasing *n*-hexane content and at constant corrole concentration (c = 1–5 × 10^{-5} M). Unfortunately, in this case no specific deviation from the behavior described above was evidenced. This is likely due to the concentration level needed for the spectroscopic analysis, at which the dimeric species do not form in sufficient quantity and its features are hidden by the most abundant monomer form, even at a $CHCl_3$/hexane 2 : 98 ratio. Thus, we have investigated the features of all corroles in methanol solutions at room temperature, upon addition of increasing amounts of water. The selection of this pair of solvents took into account the solubility properties of the macrocycles, which efficiently dissolved in methanol but not in water, and the high degree of miscibility of the two solvents. It should be noted that in this mixture the self-assembly process is probably different from that evidenced in the crystal structure, but it can anyway help to shine light on the aggregation mechanism for this series of corroles. The absorption and emission spectra of mixed methanol–water solutions of corroles **3**, **7**, and **9** at increasing content of water are reported in Fig. S6–S8 (ESI‡). The so-called critical water percentage fell around 40–50% for all the corroles and represented the point of drastic change in absorbance and emission intensity (Fig. 5 and Fig. S9, ESI‡). At water content >40–50%, a decrease, broadening and slight blue-shift (*ca.* 2 nm) of the Soret band were evident together with simultaneous lowering of the Q bands and a drastic emission quenching (Fig. S10–S12, ESI‡). Moreover, in the absorption spectra the decrease of the B and Q band intensities occurred in tandem with the appearance of at least two isosbestic points (at around 435 and 495 nm), a

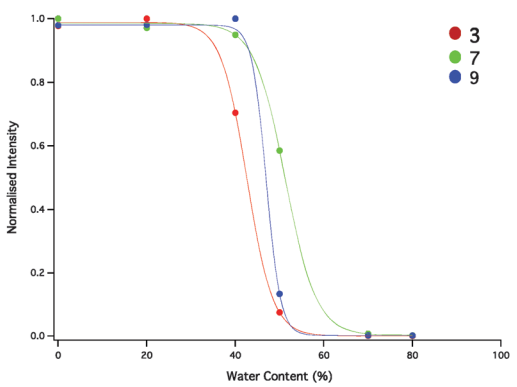

Fig. 5 Emission intensity variation at λ_{max} of corroles **3**, **7** and **9** in methanol–water mixtures (the full line is only intended as a guide for the eye and do not correspond to a model).

clear indication that absorption changes were not mere solvent effects but accounted for the appearance of a new species.

Further information about the nature of the aggregates has been gained from the luminescence lifetime analysis. Upon increasing the water content, the luminescence decay curves remained mono-exponential and the excited state lifetimes remained constant, even for almost completely quenched samples (Table S4, ESI‡). This behavior indicated that the formed aggregates were non-luminescent and the measured lifetimes were related to the fluorescence of the remaining monomer species in solution. Excitation spectra also confirmed such evaluation, keeping the features of the monomer invariant at every methanol/water ratio. This outcome differed from the stretched exponential decay behavior observed when large aggregates originate from initially small clusters.[8]

In conclusion, the character of the internal NH at the corroles's core (serving as the hydrogen bond donor) is directly responsible for the strong self-organizing properties of these compounds. When combined with the special nature of the –CONH– group, these donating properties lead to the formation of aggregates in the solid state. In solution, UV-vis absorption and fluorescence analyses revealed the formation of large aggregates in methanol–water mixtures at a critical water percentage of about 40–50%. The formation of strong intermolecular hydrogen bonds was clearly visible in crystallographic structures as well as in ^{1}H NMR spectra as strong upfield shifts of the amide-arm signals. The nature of hydrogen-bonded assembly can be regulated *via* the presence of an additional hydrogen-bond acceptor at the amide arm, opening interesting perspectives for the applications for the reported corroles.

We thank Polish NSC (844/N-ESF-EuroSolarFuels/10/2011/0) and the Italian National Research Council (CNR) in the framework of the ESF (ESF-EUROCORES-EuroSolarFuels-10-FP-006) SOLARFUELTANDEM project. The CNR PM.P04.010 MACOL project is also acknowledged.

Notes and references

1 F. Würthner, T. E. Kaiser and C. R. Saha-Möller, *Angew. Chem., Int. Ed.*, 2011, **50**, 3376.
2 For selected papers see: (*a*) S. S. Babu and D. Bonifazi, *ChemPlusChem*, 2014, **79**, 895; (*b*) T. S. Balaban, H. Tamiaki and A. R. Holzwarth, *Supermolecular Dye Chemistry*, 2005, **1**, 1–38; (*c*) G. De Luca, A. Romeo, V. Villari, N. Micali, I. Foltran, E. Foresti, I. G. Lesci, N. Roveri, T. Zuccheri and L. M. Scolaro, *J. Am. Chem. Soc.*, 2009, **131**, 6920; (*d*) M. A. Castriciano, A. Romeo, G. De Luca, V. Villari, L. M. Scolaro and N. Micali, *J. Am. Chem. Soc.*, 2011, **133**, 76; (*e*) C. Röger, Y. Miloslavina, D. Brunner, A. R. Holzwarth and F. Würthner, *J. Am. Chem. Soc.*, 2008, **130**, 5929; (*f*) T. Marangoni and D. Bonifazi, *Nanoscale*, 2013, **5**, 8837.
3 (*a*) D. A. Bryant, A. R. Holzwarth and H. J. M. Groot, *Proc. Natl. Acad. Sci. U. S. A.*, 2009, **106**, 8525; (*b*) T. S. Balaban, *Acc. Chem. Res.*, 2005, **38**, 612.
4 (*a*) T. S. Balaban, M. Linke-Schaetzel, A. D. Bhise, N. Vanthuyne, C. Roussel, C. E. Anson, G. Buth, A. Eichhöfer, K. Foster, G. Garab, H. Gliemann, R. Goddard, T. Javorfi, A. K. Powell, H. Rösner and T. Schimmel, *Chem. – Eur. J.*, 2005, **11**, 2267; (*b*) C. Chappaz-Gillot, P. L. Marek, B. J. Blaive, G. Canard, J. Bürck, G. Garab, H. Hahn, T. Jávorfi, L. Kelemen, R. Krupke, D. Mössinger, P. Ormos, C. M. Reddy, C. Roussel, G. Steinbach, M. Szabó, A. S. Ulrich, N. Vanthuyne, A. Vijayaraghavan, A. Zupcanova and T. S. Balaban, *J. Am. Chem. Soc.*, 2012, **134**, 944.
5 G. Charalambidis, E. Kasotakis, T. Lazarides, A. Mitraki and A. G. Coutsolelos, *Chem. – Eur. J.*, 2011, **17**, 7213.
6 (*a*) R. Paolesse, in *The Porphyrin Handbook*, ed. K. M. Kadish, K. M. Smith and R. Guilard, Academic Press, New-York, 2000, vol. 2, p. 201; (*b*) S. Nardis, D. Monti and R. Paolesse, *Mini-Rev. Org. Chem.*, 2005, **2**, 355; (*c*) L. Flamigni and D. T. Gryko, *Chem. Soc. Rev.*, 2009, **38**, 1635; (*d*) I. Aviv and Z. Gross, *Chem. – Eur. J.*, 2008, **14**, 3995.
7 (*a*) Z. Gross, N. Galili and I. Saltsman, *Angew. Chem., Int. Ed.*, 1999, **38**, 1427; (*b*) R. Paolesse, S. Nardis, F. Sagone and R. G. Khoury, *J. Org. Chem.*, 2001, **66**, 550; (*c*) M. Stefanelli, S. Nardis, L. Tortora, F. R. Fronczek, K. M. Smith, S. Licoccia and R. Paolesse, *Chem. Commun.*, 2011, **47**, 4255; (*d*) A. E. Meier-Callahan, A. J. Di Bilio, L. Simkhovich, A. Mahammed, I. Goldberg, H. B. Gray and Z. Gross, *Inorg. Chem.*, 2001, **40**, 6788; (*e*) Z. Gross, *J. Biol. Inorg. Chem.*, 2001, **6**, 733; (*f*) B. Ramdhanie, C. L. Stern and D. P. Goldberg, *J. Am. Chem. Soc.*, 2001, **123**, 9447; (*g*) S. Szymański, P. Paluch, D. T. Gryko, A. Nowak-Król, W. Bocian, J. Sitkowski, B. Koszarna, J. Śniechowska, M. J. Potrzebowski and L. Kozerski, *Chem. – Eur. J.*, 2014, **20**, 1720; (*h*) G. Pomarico, A. Vecchi, F. Mandoj, O. Bortolini, D. O. Cicero, P. Galloni and R. Paolesse, *Chem. Commun.*, 2014, **50**, 4076; (*i*) S. Ooi, T. Tanaka, K. H. Park, S. Lee, D. Kim and A. Osuka, *Angew. Chem., Int. Ed.*, 2015, **54**, 3107.
8 M. Stefanelli, D. Monti, M. Venanzi and R. Paolesse, *New J. Chem.*, 2007, **31**, 1722.
9 M. Seo, J. Park and S. Y. Kim, *Org. Biomol. Chem.*, 2012, **10**, 5332.
10 (*a*) I. Huc, *Eur. J. Org. Chem.*, 2004, 17; (*b*) T. Qi, V. Maurizot, H. Noguchi, T. Charoenraks, B. Kauffmann, M. Takafuji, H. Ihara and I. Huc, *Chem. Commun.*, 2012, **48**, 6337.
11 (*a*) B. Xia, D. Bao, S. Upadhyayula, G. Jones II and V. I. Vullev, *J. Org. Chem.*, 2013, **78**, 1994; (*b*) D. Bao, S. Upadhyayula, J. M. Larsen, B. Xia, B. Georgieva, V. Nuñez, E. M. Espinoza, J. D. Hartman, M. Wurch, A. Chang, C.-K. Lin, J. Larkin, K. Vasquez, G. J. O. Beran and V. I. Vullev, *J. Am. Chem. Soc.*, 2014, **136**, 12966.
12 B. Koszarna and D. T. Gryko, *J. Org. Chem.*, 2006, **71**, 3707.
13 D. T. Gryko, P. Piątek and J. Jurczak, *Tetrahedron*, 1997, **53**, 7957.
14 (*a*) D. T. Gryko, P. Piątek and J. Jurczak, *Synthesis*, 1999, 336; (*b*) K. ó Proinsias, M. Giedyk, G. I. Sharina, E. Martin and D. Gryko, *ACS Med. Chem. Lett.*, 2012, **3**, 476; (*c*) H. Morimoto, R. Fujiwara, Y. Shimizu, K. Morisaki and T. Ohshima, *Org. Lett.*, 2014, **16**, 2018; (*d*) D. T. Gryko, D. Gryko and J. Jurczak, *Synlett*, 1999, 1310.
15 (*a*) T. Hori and A. Osuka, *Eur. J. Org. Chem.*, 2010, 2379; (*b*) F. Faschinger, S. Aichhorn, M. Himmelsbach and W. Schoefberger, *Synthesis*, 2014, 3085.
16 (*a*) R. Paolesse, F. Sagone, A. Macagnano, T. Boschi, L. Prodi, M. Montalti, N. Zaccheroni, F. Bolletta and K. M. Smith, *J. Porphyrins Phthalocyanines*, 1999, **3**, 364; (*b*) R. Paolesse, A. Marini, S. Nardis, A. Froiio, F. Mandoj, D. J. Nurco, L. Prodi, M. Montalti and K. M. Smith, *J. Porphyrins Phthalocyanines*, 2003, **7**, 25; (*c*) A. Ghosh, T. Wondimagegn and A. B. J. Parusel, *J. Am. Chem. Soc.*, 2000, **122**, 5100.
17 (*a*) B. Ventura, A. Degli Esposti, B. Koszarna, D. T. Gryko and L. Flamigni, *New J. Chem.*, 2005, **29**, 1559; (*b*) T. H. Ngo, F. Puntoriero, F. Nastasi, K. Robeyns, L. Van Meervelt, S. Campagna, W. Dehaen and W. Maes, *Chem. – Eur. J.*, 2010, **16**, 5691.
18 (*a*) M. Stefanelli, G. Pomarico, L. Tortora, S. Nardis, F. R. Fronczek, G. T. McCandless, K. M. Smith, M. Manowong, Y. Fang, P. Chen, K. M. Kadish, A. Rosa, G. Ricciardi and R. Paolesse, *Inorg. Chem.*, 2012, **51**, 6928; (*b*) D. Gao, G. Canard, M. Giorgi and T. S. Balaban, *Eur. J. Inorg. Chem.*, 2012, 5915.
19 (*a*) M. Kruk, T. H. Ngo, P. Verstappen, A. Starukhin, J. Hofkens, W. Dehaen and W. Maes, *J. Phys. Chem. A*, 2012, **116**, 10695; (*b*) W. Beenken, M. Presselt, T. H. Ngo, W. Dehaen, W. Maes and M. Kruk, *J. Phys. Chem. A*, 2014, **118**, 862.